BIOCHEMISTRY
including biophysical chemistry & molecular biology

Article

pubs.acs.org/biochemistry

Mechanism of the Novel Prenylated Flavin-Containing Enzyme Ferulic Acid Decarboxylase Probed by Isotope Effects and Linear Free-Energy Relationships

Kyle L. Ferguson,[†] Nattapol Arunrattanamook,[‡,†] and E. Neil G. Marsh*[,†,§]

[†]Department of Chemistry, [‡]Department of Chemical Engineering, and [§]Department of Biological Chemistry, University of Michigan, Ann Arbor, Michigan 48109, United States

ABSTRACT: Ferulic acid decarboxylase from *Saccharomyces cerevisiae* catalyzes the decarboxylation of phenylacrylic acid to form styrene using a newly described prenylated flavin mononucleotide cofactor. A mechanism has been proposed, involving an unprecedented 1,3-dipolar cyclo-addition of the prenylated flavin with the $\alpha{=}\beta$ bond of the substrate that serves to activate the substrate toward decarboxylation. We measured a combination of secondary deuterium kinetic isotope effects (KIEs) at the α- and β-positions of phenylacrylic acid together with solvent deuterium KIEs. The solvent KIE is 3.3 on V_{max}/K_M but is close to unity on V_{max}, indicating that proton transfer to the product occurs before the rate-determining step. The secondary KIEs are normal at both the α- and β-positions but vary in magnitude depending on whether the reaction is performed in H_2O or D_2O. In D_2O, the enzyme catalyzed the exchange of deuterium into styrene; this reaction was dependent on the presence of bicarbonate. This observation implies that CO_2 release must occur after protonation of the product. Further information was obtained from a linear free-energy analysis of the reaction through the use of a range of *para*- and *meta*-substituted phenylacrylic acids. Log(k_{cat}/K_M) for the reaction correlated well with the Hammett σ^- parameter with $\rho = -0.39 \pm 0.03$; $r^2 = 0.93$. The negative ρ value and secondary isotope effects are consistent with the rate-determining step being the formation of styrene from the prenylated flavin−product adduct through a cyclo-elimination reaction.

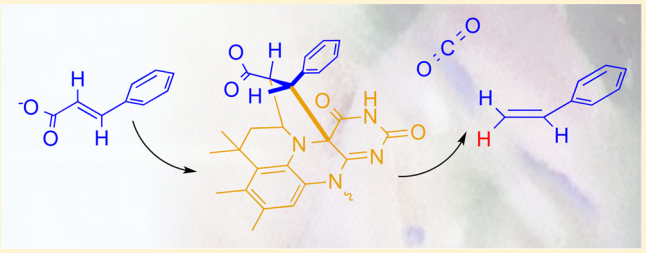

Enzyme-catalyzed decarboxylation reactions constitute an important class of biological reactions yet are inherently difficult to achieve under physiological conditions.[1,2] This is due to the accumulation of negative charge on the α-carbon in the transition state of decarboxylation, which results in a high-energy transition state. To overcome the unfavorable energetic barrier for decarboxylation enzymes, a wide variety of cofactors can be employed, including organic prosthetic groups such as thiamine pyrophosphate and pyridoxal phosphate and Lewis acids such as Mg^{2+}, Fe^{2+}, and Mn^{2+}, which serve to stabilize the negative charge.[1,2]

Decarboxylases have also attracted interest as industrial-scale catalysts for the production of high value, optically pure chemicals under mild conditions in environmentally friendly bioprocesses.[3,4] Aromatic acid decarboxylases are of particular interest, as these enzymes can be used to produce a wide variety of commercially valuable substituted aromatic compounds such as styrene, vinyl guiacol, and vanillin. One such enzyme, ferulic acid decarboxylase (FDC), catalyzes the decarboxylation of a wide variety of ring-substituted phenylacrylic acid (cinnamic acid) derivatives to produce the corresponding substituted styrene derivatives.[5−7]

Recently, studies on FDC have identified a new flavin-derived cofactor involved in the decarboxylation of α,β-unsaturated carboxylic acids.[7−9] This cofactor, which has been termed a prenylated (pr) flavin, is a modified form of FMN (prFMN) containing an extra 6-membered ring formed by the addition of an isopentyl group between the N5 and C6 positions of the isoalloxazine flavin nucleus (Figure 1). The cofactor is used by a family of enzymes represented by UbiD, which catalyzes the decarboxylation of 4-hydroxy-3-octaprenylbenzoic acid as part of ubiquinone biosynthesis in many prokaryotes.[10−14] PrFMN was recently shown to be synthesized from dimethylallyl phosphate and FMN by UbiX.[8,9]

On the basis of crystallographic evidence, a mechanism has been proposed for FDC that involves an initial 1,3-dipolar cycloaddition between prFMN and the double bond of phenylacrylic acid, which is followed by a Grob-type elimination of carbon dioxide (Figure 1A).[8,15−17] Protonation of the substrate by an active site glutamate and finally cyclo-elimination to yield styrene and prFMN complete the catalytic cycle. The mechanism of FDC is of considerable interest because true thermal pericyclic reactions are extremely rare in enzymes, and 1,3-dipolar cycloadditions are unprecedented.[18,19] We note that a simpler mechanism involving a Michael addition of prFMN to the double bond of phenylacrylic acid followed by decarboxylation and elimination of the cofactor was also considered (Figure 1B).[8] However, this mechanism was disfavored on the basis of an X-ray structure of a covalent inhibitor−prFMN adduct that was inconsistent with prFMN reacting in this way.[8] Here, we used a combination of

Received: February 23, 2016
Revised: April 26, 2016

DOI: 10.1021/acs.biochem.6b00170
Biochemistry XXXX, XXX, XXX−XXX

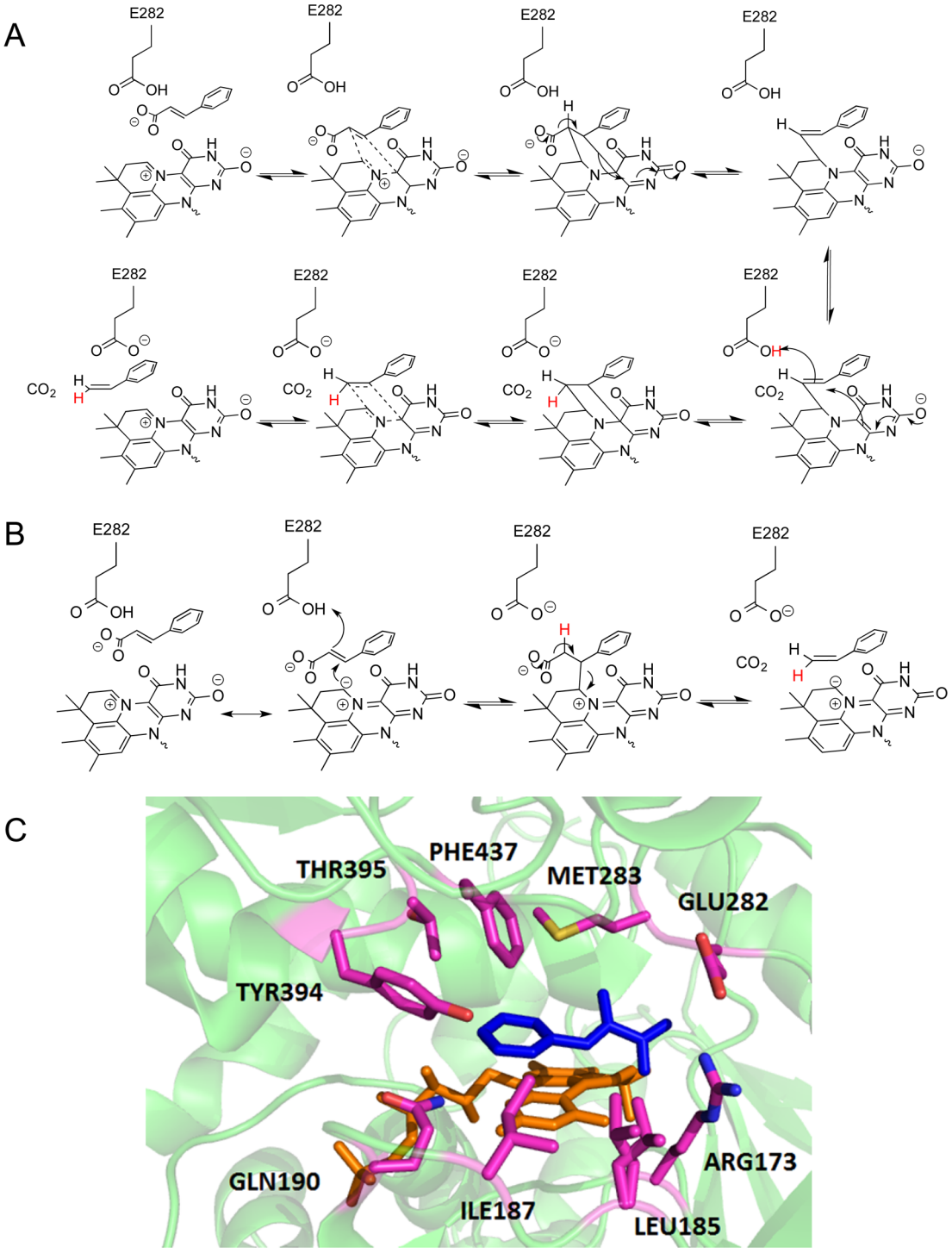

Figure 1. Proposed mechanisms for the FDC-catalyzed decarboxylation of phenylacrylic acid proceeding through (A) 1,3-dipolar cyclo-addition to the prFMN cofactor and (B) Michael addition/elimination of prFMN to the substrate. (C) Details of the active site: active site residues are shown in magenta with the prFMN cofactor in orange. The substrate analogue α-methylphenylacrylic acid (blue) is shown bound in the active site (PDB ID: 4ZA7).

isotope effects and linear free-energy analysis to probe the mechanism by which this newly discovered cofactor catalyzes decarboxylation reactions.

MATERIALS AND METHODS

Materials. *trans*-Cinnamic acid, styrene, *p*-coumaric acid, 4-methoxycinnamic acid, 4-fluorocinnamic acid, 4-formylcinnamic acid, 4-bromocinnamic acid, 4-chlorocinnamic acid, and 4-methylcinnamic acid were purchased from Acros Organic. *trans*-Cinnamic acid, 3-nitrocinnamic acid, and 3-methoxycinnamic acid were purchased from Sigma-Aldrich. 4-Cyanocinnamic acid was purchased from Matrix Scientific. 4-Aminocinnamic acid and 4-nitrocinnamic acid were purchased from Tokyo Chemical Industries. 4-(2-Carboxy-vinyl)-benzoic acid methyl ester was purchased from Santa Cruz Biotechnology. All other chemicals were purchased from Sigma-Aldrich.

DOI: 10.1021/acs.biochem.6b00170
Biochemistry XXXX, XXX, XXX−XXX

d_7-*trans*-Cinnamic acid and 3-d_1-*trans*-cinnamic acid were purchased from Sigma-Aldrich; 2-d_1-*trans*-cinnamic acid was synthesized by reaction of benzaldehyde with d_6-acetic anhydride using standard literature procedures.[20]

Holo-FDC was recombinantly expressed in *Escherichia coli* and purified as described previously.[7]

Enzyme Assay. Assays of FDC activity were routinely performed in 100 mM phosphate buffer (pH 7.4) at 25 °C. Stock solutions of substrates were prepared in DMSO. Assays contained substrates at various initial concentrations between 10 and 50 μM. Reactions were initiated by addition of FDC to a final concentration between 50 and 500 nM depending on the activity of the enzyme with a particular substrate. We followed the activity spectrophotometrically by monitoring depletion of the substrates. The wavelengths used to monitor the enzyme activity and extinction coefficients of the various substrates are given in Table 1. Care was taken to ensure that the assay remained linear at the concentrations of substrate and enzyme used.

Table 1. Assay Wavelengths and Extinction Coefficients for Phenylacylic Acid Derivatives Used in This Study

substituent	assay wavelength (nm)	$\varepsilon_{substrate}$ (M^{-1} cm^{-1})	$\varepsilon_{product}$ (M^{-1} cm^{-1})
p-NH_2–	292	17900	1840
p-HO–	294	16900	7930
p-CH_3O–	290	18900	5410
p-CH_3–	280	19000	
p-H–	276	17900	
p-F–	276	14300	948
m-CH_3O–	276	14300	
p-Cl–	280	21200	1810
p-Br–	278	22000	2630
p-CH_3OOC–	300	19000	
m-NO_2–	280	14800	7240
p-CN–	284	26600	7230
p-CHO–	304	24800	
p-NO_2–	314	18000	9760

pH Dependence and Solvent and Secondary Deuterium Isotope Effect Measurements. The pH dependence of FDC activity was studied with the following buffers: pH 4.0–6.5, 100 mM sodium citrate; pH 6.5–8.0, 100 mM sodium phosphate; pH 8.0–9.0, 100 mM Tris chloride. For measurements in deuterated solvents, the buffer components were dissolved in D_2O (99.9%) and repeatedly lyophilized to exchange protium. pD was corrected using eq 1, where χ is the mole fraction of D_2O.

$$pD = pH + 0.076\chi^2 + 0.3314\chi + 0.00009 \quad (1)$$

To measure the solvent deuterium kinetic isotope effect on styrene formation, the reactions were performed in buffers containing various mole fractions of D_2O, and the deuterium content of the styrene produced was analyzed by GC-MS as described previously.[17,21]

Secondary KIEs were measured at substrate concentrations of 50 μM and enzyme concentrations of 50 nM so that the measurements represent the KIE on V_{max}/K_M. Experiments were performed at a pD and pH of 6.5, where the activity of the enzyme is independent of pH.

We monitored the proton exchange experiments using ^{1}H NMR at 400 MHz at 22 °C by monitoring the disappearance of the styrene resonance at 5.2 ppm. The reaction buffer was comprised of 100 mM potassium citrate in D_2O (pD 6.5), 10 μM FDC, 20 mM $KHCO_3$, and 2.5 mM styrene. Reaction mixtures that lacked $KHCO_3$ were also prepared and were degassed prior to reaction to remove dissolved CO_2.

RESULTS

Hammett Analysis of FDC. Linear free-energy relationships provide a powerful tool with which to interrogate reaction mechanisms.[22] The narrow substrate range of most enzymes limits the utility of this approach for the investigation of enzyme reactions, although for more promiscuous enzymes, linear free-energy analyses have proved to be highly informative.[23−25] The broad substrate range of FDC made it an excellent candidate to conduct a Hammett analysis of the decarboxylation reaction. The kinetics of decarboxylation were studied for a series of 14 *para*- and *meta*-substituted phenylacrylic acids with σ^- values ranging from 1.25 to −0.66, which are listed in Table 2.

Table 2. k_{cat}/K_M Values Measured for FDC-Catalyzed Decarboxylation of Various Phenylacrylic Acid Derivatives

substituent	σ^-	k_{cat}/K_M (M^{-1} s^{-1})	$\log(k_{cat}/K_M)$
p-NH_2–	−0.66	12400 ± 670	4.09 ± 0.023
p-HO–	−0.37	4550 ± 250	3.66 ± 0.023
p-CH_3O–	−0.27	28100 ± 1800	4.45 ± 0.027
p-CH_3–	−0.17	27000 ± 1600	4.43 ± 0.025
p-H–	0	24500 ± 1400	4.39 ± 0.023
p-F–	0.02	27500 ± 1800	4.44 ± 0.027
m-CH_3O–	0.12	27000 ± 2000	4.44 ± 0.031
p-Cl–	0.23	19700 ± 1200	4.29 ± 0.026
p-Br–	0.26	21400 ± 1300	4.33 ± 0.026
p-CH_3OOC–	0.66	11500 ± 320	4.06 ± 0.012
m-NO_2–	0.71	14300 ± 1000	4.16 ± 0.030
p-CN–	0.88	12800 ± 880	4.11 ± 0.029
p-CHO–	1.13	8690 ± 300	3.88 ± 0.015
p-NO_2–	1.25	8690 ± 160	3.94 ± 0.008

The relatively high K_M values for some substrates of >0.35 mM precluded reliable measurements of full Michaelis–Menten curves. Therefore, initial velocities were measured at low substrate concentrations relative to K_M, where velocity is proportional to substrate concentration, allowing the determination of k_{cat}/K_M for each substrate (Table 2).

The resulting Hammett plot for a series of 12 of the substituted phenylacrylic acids listed in Table 2 is shown in Figure 2. The data were poorly correlated with the standard Hammett parameter σ ($\rho = -0.5$; $r^2 = 0.65$) but showed a strong correlation with the Hammett parameter σ^- ($\rho = -0.39 \pm 0.03$; $r^2 = 0.93$). Two substrates, 4-amino- and 4-hydroxyphenylacrylic acid, reacted much more slowly than expected based on their highly negative σ^- values. These substrates are the only compounds that contain hydrogen bond-donating functional groups. Although it is unclear why they react so slowly, the large deviation of these compounds from the trend line suggests they may react by a different mechanism. For this reason, they were excluded from the calculation of ρ in our analysis.

The apparent linearity of the Hammett analysis provides strong evidence that a chemical step is rate-determining in the reaction. The negative slope of the plot, which is caused by electron-releasing groups that increase the rate of reaction, is very unusual, as decarboxylation reactions (both enzymatic and nonenzymatic) involve a buildup of negative charges in the transition state and are therefore associated with large positive ρ values. The strong correlation with σ^- indicates that, in addition to inductive effects, delocalization of electrons through the extended

DOI: 10.1021/acs.biochem.6b00170
Biochemistry XXXX, XXX, XXX–XXX

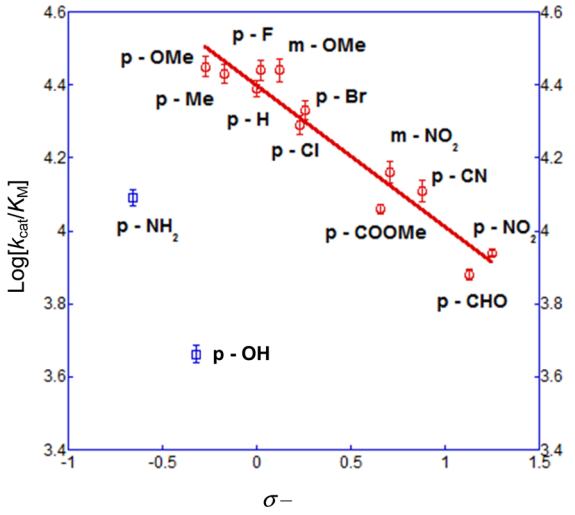

Figure 2. Hammett plot for the FDC-catalyzed decarboxylation of 14 different *para*- and *meta*-substituted phenylacrylic acids. Data points in red were used to determine ρ; the two outliers in blue were excluded from the analysis.

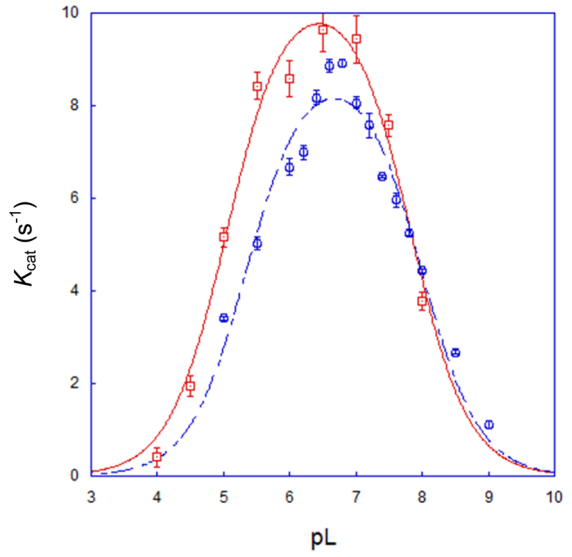

Figure 3. pL-rate profile for decarboxylation of phenylacylic acid by FDC in H_2O (blue) and D_2O (red) buffers.

π-system associated with the aromatic ring is important in stabilization of the transition state in a step that contributes significantly to the overall rate of the reaction.[19,25]

Kinetic Isotope Effects. The proposed mechanism of the FDC reaction involves the creation and breaking of bonds at three carbon atoms in the substrate. The kinetic significance of these bonding changes in the overall reaction was examined through the use of kinetic isotope effects. In particular, proton incorporation into styrene should be subject to a solvent kinetic isotope effect, and the transient changes in hybridization at Cα and Cβ of the substrate should be subject to secondary kinetic isotope effects.

pH Dependence and Solvent Isotope Effects. Initial characterization by ^{1}H NMR of the styrene produced in the FDC reaction established that the solvent proton is incorporated *trans* to the phenyl ring of styrene, as evidenced by the disappearance of the signal at 5.2 ppm when the reaction was performed in D_2O (see Deuterium Exchange into Styrene). Therefore, decarboxylation occurs with the retention of the configuration at Cα, which is in accord with the geometry of the active site and the proposed role of Glu282 acting as the proton donor.

Because solvent isotope effects may be influenced by pH, we first investigated the activity of FDC as a function of pH and pD. Under V_{max} conditions, the enzyme exhibits a bell-shaped pH dependence, typical of many enzymes, with an activity maximum at pH 6.5. The acidic limb is characterized by pK_a = 5.3 ± 0.1, and the basic limb is characterized by pK_a = 8.0 ± 0.1. The enzyme activity in deuterated buffers was very similar, although the pK_a of the acidic limb was shifted to a slightly lower value (pK_a = 5.0 ± 0.1) (Figure 3). On the basis of the pL curves, the solvent KIE on V_{max} ($^DV_{solvent}$) was measured at pL = 6.5. The value is very close to unity ($^DV_{solvent}$ = 0.95 ± 0.05; n = 5), indicating that proton transfer to the product is not a kinetically significant step in the overall reaction.

To investigate the protonation step in more detail, we conducted a proton inventory analysis, which allowed us to measure the solvent KIE on V_{max}/K_M ($^DV/K_{solvent}$). Reaction mixtures were set up at pL 6.5 in buffers containing 0.1 mole fraction increments of deuterium (χ_{D_2O}). The styrene produced by the reaction was isolated, and the mole fraction of deuterium ($\chi_{styrene}$) was determined by GC-MS. While $^DV/K_{solvent}$ may be estimated by the determination of $\chi_{styrene}$ at χ_{D_2O} = 0.5, for which $^DV/K_{solvent}$ = ~3.3,

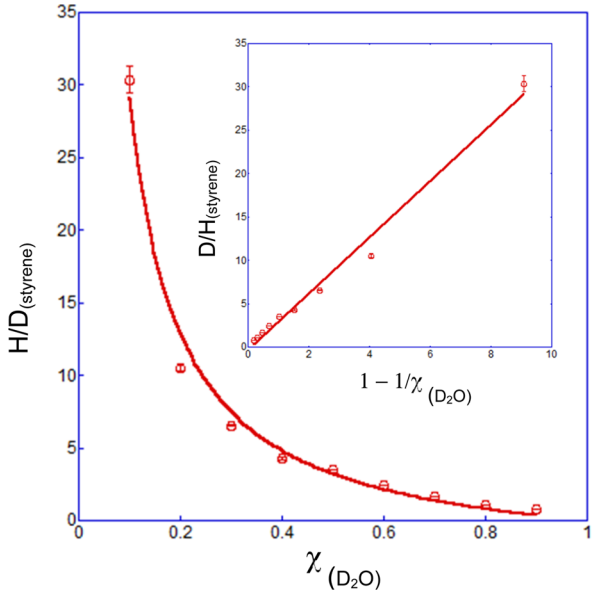

Figure 4. Proton inventory for FDC. The mole fraction of D_2O in the solvent is plotted against the ratio of protiated to deuterated styrene. The solid line represents the best fit to eq 2. A linearized plot of the data is shown in the inset.

we can determine it more accurately by fitting the full proton inventory data, shown in Figure 4, to eq 2.

$$\chi_{product} = {}^{D_2O}SIE_{obs}\left(\frac{1}{\chi_{solvent}} - 1\right) \quad (2)$$

From this analysis, a substantial solvent KIE on V_{max}/K_M is evident, with $^DV/K_{solvent}$ = 3.33 ± 0.09. We note that eq 2 assumes that only a single proton is in motion in the transition state; the excellent fit of the data to the equation suggests that this assumption is valid. KIEs on V_{max} are observed only if the isotopically sensitive step is rate-determining under saturating substrate concentrations, whereas the KIE on V_{max}/K_M represents the KIE determined at low substrate concentrations and reflects all steps up to and including the first irreversible step.

DOI: 10.1021/acs.biochem.6b00170
Biochemistry XXXX, XXX, XXX−XXX

Our data therefore indicate that the steps that control V_{max}/K_M and V_{max} are different. We interpret these results as an indication that protonation of the product is associated with a significant energetic barrier and occurs before the first irreversible rate-determining step of the reaction. As discussed below, these steps are likely associated with release of the products from the enzyme.

Secondary Kinetic Isotope Effects. Secondary kinetic isotope effects report on changes in the stiffness of bonds adjacent to the site of the reaction and may be either normal or inverse.[26−29] They are particularly informative for an examination of changes in the geometry of carbon atoms: the transition from tetrahedral to planar geometry is associated with a normal secondary KIE, whereas the transition from planar to tetrahedral geometry is associated with an inverse secondary KIE. To investigate the mechanism of the FDC reaction, we measured secondary deuterium KIEs at both the α- and β-positions of phenylacrylic acid in both D_2O and H_2O buffers (the commercially available β-deuterated phenylacrylic acid was also deuterated on the phenyl ring; the remote isotope was assumed to not influence the KIE at the β-position). KIEs were determined at 25 °C in 100 mM sodium citrate buffer (pL 6.5) by a direct comparison of reaction rates at low substrate concentrations relative to K_M so that the measurements represent KIEs on V_{max}/K_M. The data are presented in Table 3.

Table 3. Summary of Secondary Kinetic Isotope Effects Measured for the FDC-Catalyzed Decarboxylation of Deuterated Phenylacrylic Acids in H_2O and D_2O

deuterium position	$2° {}^{D}V/K$ (H_2O)	$2° {}^{D}V/K$ (D_2O)
Cα	0.99 ± 0.02	1.12 ± 0.030
Cβ	1.10 ± 0.016	1.01 ± 0.027
Cα and Cβ	1.15 ± 0.017	1.32 ± 0.035

In H_2O, no apparent 2° KIE was observed at the α-position, whereas at the β-position a large, normal 2° KIE was measured ($^{2o D}V/K_{\beta(H_2O)}$ = 1.10 ± 0.03; n = 9). In contrast, in D_2O, the apparent 2° KIE at the α-position became significant ($^{2o D}V/K_{\alpha(D_2O)}$ = 1.12 ± 0.03; n = 9), whereas the 2° KIE at the β-position was suppressed and was at unity within error. When dideuterated phenylacrylic acid was the substrate, large 2° KIEs were measured in both H_2O and D_2O. The fact that these KIEs are normal indicates that they both arise from the rehybridization of the α- and β-carbons from tetrahedral to planar geometry during the reaction.

Deuterium Exchange into Styrene. The decarboxylation catalyzed by FDC can be driven in the reverse direction in the presence of styrene and high concentrations of bicarbonate.[30] We used the reversibility of the reaction to examine the requirements for proton transfer between Glu282 and substrate. Reaction mixtures were set up in citrate-buffered D_2O solutions containing 2 mM styrene that were either purged of dissolved CO_2 or supplemented with 20 mM $KHCO_3$. We monitored the exchange of deuterium into styrene using ^1H NMR by following the disappearance of the resonance at 5.20 ppm. Deuterium incorporation at the *trans*-position of C1 also resulted in a simplification of the signal at 5.75 ppm due to the *cis*-C1 hydrogen from a doublet of doublets to a doublet together with a slight upfield isotope-induced chemical shift. In CO_2-purged buffers, little to no exchange of deuterium was observed (Figure 5), whereas the addition of $KHCO_3$ resulted in deuterium exchange into styrene occurring quite rapidly with an apparent rate constant k_{app} of ∼1.5 min^{-1}. This result demonstrates that CO_2 must be present in the active site for protonation/deprotonation of the styrene−prFMN adduct to occur. This implies that dissociation of CO_2 does not occur until after the product is protonated when the reaction proceeds in the decarboxylation direction.

DISCUSSION

The novel isopentenyl modification of FMN converts a cofactor generally associated with redox reactions into one that supports decarboxylation. Its discovery raises a number of interesting questions regarding the mechanism by which FDC catalyzes the decarboxylation of aromatic substrates and the nature of the rate-determining step. The proposed mechanism involving a 1,3-dipolar cyclo-addition of prFMN with phenylacrylic acid (Figure 1A) seems plausible, as the alkylation of N6 of the flavin introduces functionality into the cofactor which is expected to have an ylide character similar to that of an azomethine ylide.[8,31] The kinetic experiments described here provide insight into the rate-determining step in the reaction mechanism and provide further lines of support for the mechanistic proposal shown in Figure 1, which is based primarily on X-ray crystallography of enzyme−inhibitor complexes.

The stereospecificity with which deuterium is incorporated into styrene is consistent with the α-carbon remaining bonded to prFMN after decarboxylation. If the α-carbon of the substrate was free to rotate about the Cα−Cβ bond, then a scrambling of the isotope would be observed. The stereochemistry of deuterium incorporation, which occurs with a retention of the configuration, is also consistent with the proposed role of Glu282 acting as the proton donor in the reaction. The basic limb of the pH-rate profile (Figure 3), which is characterized by an apparent pK_a of 8.0, may be attributed to Glu282, as this residue must be protonated for the reaction to proceed. Although a pK_a of 8.0 is quite high even for a buried glutamate side chain, the proximity of the negatively charged substrate is expected to further raise its pK_a.

Furthermore, the observation that proton exchange into styrene requires HCO_3^- indicates that release of CO_2 from the enzyme must occur after proton transfer to the substrate (we assume that HCO_3^- serves as a CO_2 source rather than the enzyme utilizing HCO_3^- directly). It would also be consistent if the proton transfer preceded decarboxylation in the reaction mechanism, although this seems unlikely. Lastly, the large solvent deuterium KIE on V_{max}/K_M ($^{D}V/K_{solvent}$ = 3.33 ± 0.09), measured by internal competition, contrasts with the KIE on V_{max}, measured by a direct comparison of reaction rates in H_2O and D_2O, which are close to unity. This is consistent with protonation of the styrene−prFMN adduct being the rate-determining step in the decarboxylation/protonation portion of the reaction. However, it is unlikely that protonation is the rate-determining step that limits k_{cat}. This would be inconsistent with the fact that the solvent KIE on V_{max} is unity and that the secondary KIEs are normal, rather than inverse, as discussed below.

The strong correlation of $\log(k_{cat}/K_M)$ with the Hammett σ^- parameter (Figure 2) points to a chemical step in the reaction as rate-determining, rather than a substrate-binding or product release step, in which case ρ would be expected to be close to zero. Interestingly and unexpectedly, for a decarboxylation reaction, ρ is negative (ρ = −0.39). Therefore, it seems unlikely, regardless of the precise details of the mechanism, that the decarboxylation step is rate-determining. Otherwise, the buildup of negative charge in the transition state should lead to a positive ρ value, which is generally observed in decarboxylation reactions.[22,25]

The negative ρ value provides evidence that the 1,3-cyclo-elimination reaction that leads to the release of styrene from prFMN is likely to be rate-determining in the FDC reaction; this

DOI: 10.1021/acs.biochem.6b00170
Biochemistry XXXX, XXX, XXX−XXX

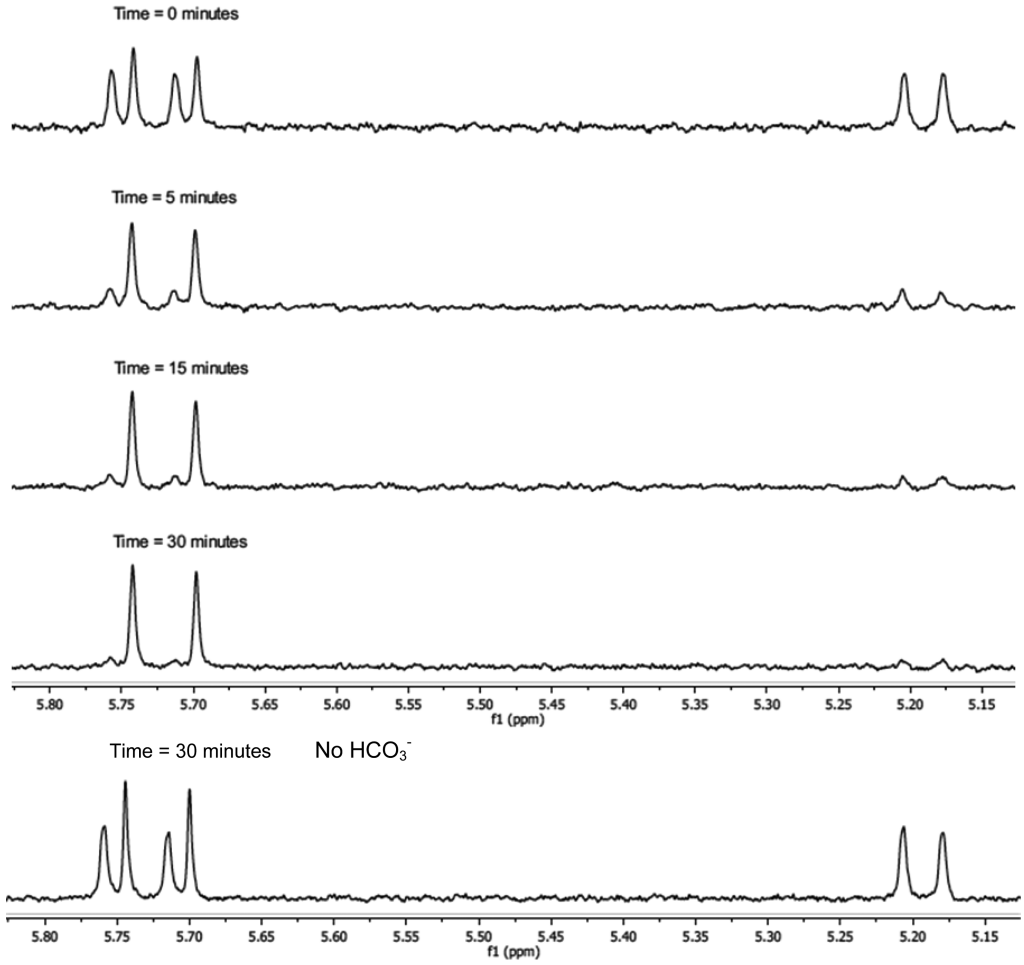

Figure 5. FDC catalyzes deuterium exchange into styrene in the presence of 20 mM HCO_3^-. ^1H NMR spectra were recorded at 500 MHz between 0 and 30 min after addition of FDC. The bottom spectrum was recorded under the same conditions but in the absence of HCO_3^-. For details, see the text.

would be consistent with the 2° KIE measurements discussed below. We note that, although the correlation of reactivity with σ^- is generally discussed in terms of resonance effects, this formalism derives from the overlap of p-orbitals to form extended π-systems and is thus correlated with the HOMO-LUMO analyses used to rationalize thermal pericyclic reactions. In 1,3-dipolar cyclo-addition reactions, azomethine ylides have a nucleophilic character and react increasingly rapidly with increasingly electron-withdrawing dipolarophiles (i.e., the rate of reaction is dominated by the difference in energy between the HOMO of the azomethine ylide and the LUMO of the dipolarophile).[31] Indeed, these types of cyclo-addition reactions have been found to exhibit linear free-energy relationships that correlate well with the electronic properties of the dipolar ylide and the dipolarophile.[31] This implies that the rate of the reverse cyclo-elimination reaction will, conversely, be slowed by electron-withdrawing substituents. In the present case, the structure of prFMN suggests that its reactivity toward dipolarophiles will resemble that of an azomethine ylide; hence, electron-withdrawing substituents on the phenyl ring will slow the final cyclo-elimination reaction leading to product formation, consistent with our experimental observations.

The 2° KIEs measured for FDC provide further evidence that a chemical step, rather than a substrate binding or product release step, is rate-determining. Normal 2° KIEs are observed at both the α- and β-positions of phenyl acrylate, although they are solvent-dependent, which complicates their interpretation as discussed below. Normal 2° isotope effects are indicative of a change in geometry at the carbon atoms from tetrahedral to planar,[27] which again points to the rate-determining step involving the formation of the styrene double bond in the final cyclo-elimination reaction.

The change in the apparent 2° KIEs observed when the reaction is performed in D_2O is unusual but may be explained by the fact that, when the α-carbon undergoes rehybridization, it contains an additional deuterium from the solvent. This will introduce a cryptic 2° KIE at the α-carbon that could mask the 2° KIE at the β-carbon. When the enzyme is reacted with α-deuterated phenylacrylic acid in D_2O, the α-carbon will contain two deuterium atoms; thus, the observed 2° KIE will be further elevated and will appear as a normal KIE. A similar argument can be made to explain the further increase in 2° KIEs when α,β-dideuterated substrates are used. The pattern of 2° KIEs further suggests that the 1,3-cyclo-elimination reaction that leads to the formation of the styrene double bond occurs in a concerted but asynchronous reaction in which bond cleavage is advanced at the α-carbon with respect to the β-carbon.

Our results do not definitively rule out a previously considered mechanism in which a Michael addition of prFMN to phenylacrylic acid facilitates decarboxylation, as shown in Figure 1B.[8] However, we consider this possibility as less likely because in this mechanism the 2° KIEs indicate that decarboxylation was rate-limiting, concomitant with a change in geometry from tetrahedral to planar at the α- and β-carbons. As discussed above, postulating decarboxylation as the rate-limiting step appears inconsistent with the negative value of ρ associated with the overall reaction.

DOI: 10.1021/acs.biochem.6b00170
Biochemistry XXXX, XXX, XXX−XXX

In conclusion, the results presented here are consistent with the proposed mechanism for FDC, which involves a novel cycloaddition reaction of the substrate with the prenylated flavin cofactor. The results suggest that the rate-determining step in the catalytic cycle is resolution of the product−prFMN adduct through a cyclo-elimination reaction. Further mechanistic studies will be necessary to better establish the timing of the decarboxylation and protonation events, for example, by the measurement of heavy atom KIEs associated with decarboxylation. So far, evidence for the cyclic adduct between the substrate and prFMN remains indirect, and further experiments are needed to substantiate the formation of this key intermediate. Our results suggest it may be possible to stabilize this adduct sufficiently to permit its characterization by reaction of the enzyme with highly electron-withdrawing substrates that slow the rate of cyclo-elimination. The substrate reactivity patterns uncovered here may also be useful in guiding efforts to engineer FDC toward alternative substrates or greater catalytic efficiency.

AUTHOR INFORMATION

Corresponding Author

*E-mail: nmarsh@umich.edu.

Funding

This research was supported in part by grants from the National Science Foundation (CHE 1152055 and CBET 1336636) to E.N.G.M.; N.A. acknowledges the support of a Royal Thai Government Scholarship.

Notes

The authors declare no competing financial interest.

ABBREVIATIONS

FDC, ferulic acid decarboxylase; prFMN, prenylated flavin mononucleotide; SIE, solvent isotope effect; KIE, kinetic isotope effect

REFERENCES

(1) Jordan, F., and Patel, H. (2013) Catalysis in Enzymatic Decarboxylations: Comparison of Selected Cofactor-Dependent and Cofactor-Independent Examples. *ACS Catal. 3*, 1601−1617.

(2) Kourist, R., Guterl, J.-K., Miyamoto, K., and Sieber, V. (2014) Enzymatic Decarboxylation-An Emerging Reaction for Chemicals Production from Renewable Resources. *ChemCatChem 6*, 689−701.

(3) Claypool, J. T., Raman, D. R., Jarboe, L. R., and Nielsen, D. R. (2014) Technoeconomic evaluation of bio-based styrene production by engineered Escherichia coli. *J. Ind. Microbiol. Biotechnol. 41*, 1211−1216.

(4) McKenna, R., Thompson, B., Pugh, S., and Nielsen, D. R. (2014) Rational and combinatorial approaches to engineering styrene production by Saccharomyces cerevisiae. *Microb. Cell Fact. 13*, 123.

(5) Huang, Z. X., Dostal, L., and Rosazza, J. P. N. (1994) Purification and Characterization of a Ferulic Acid Decarboxylase from Pseudomonas-Fluorescens. *J. Bacteriol. 176*, 5912−5918.

(6) Mukai, N., Masaki, K., Fujii, T., Kawamukai, M., and Iefuji, H. (2010) PAD1 and FDC1 are essential for the decarboxylation of phenylacrylic acids in *Saccharomyces cerevisiae*. *J. Biosci. Bioengin. 109*, 564−569.

(7) Lin, F., Ferguson, K. L., Boyer, D. R., Lin, X. N., and Marsh, E. N.G. (2015) Isofunctional enzymes PAD1 and UbiX catalyze formation of a novel cofactor required by ferulic acid decarboxylase and 4-hydroxy-3-polyprenylbenzoic acid decarboxylase. *ACS Chem. Biol. 10*, 1137−1144.

(8) Payne, K. A. P., White, M. D., Fisher, K., Khara, B., Bailey, S. S., Parker, D., Rattray, N. J. W., Trivedi, D. K., Goodacre, R., Beveridge, R., Barran, P., Rigby, S. E. J., Scrutton, N. S., Hay, S., and Leys, D. (2015) New cofactor supports alpha,beta-unsaturated acid decarboxylation via 1,3-dipolar cyclo-addition. *Nature 522*, 497−501.

(9) White, M. D., Payne, K. A. P., Fisher, K., Marshall, S. A., Parker, D., Rattray, N. J. W., Trivedi, D. K., Goodacre, R., Rigby, S. E. J., Scrutton, N. S., Hay, S., and Leys, D. (2015) UbiX is a flavin prenyltransferase required for bacterial ubiquinone biosynthesis. *Nature 522*, 502−506.

(10) Bentinger, M., Tekle, M., and Dallner, G. (2010) Coenzyme Q- Biosynthesis and functions. *Biochem. Biophys. Res. Commun. 396*, 74−79.

(11) Gulmezian, M., Hyman, K. R., Marbois, B. N., Clarke, C. F., and Javor, G. T. (2007) The role of UbiX in Escherichia coli coenzyme Q biosynthesis. *Arch. Biochem. Biophys. 467*, 144−153.

(12) Jacewicz, A., Izumi, A., Brunner, K., Schnell, R., and Schneider, G. (2013) Structural Insights into the UbiD Protein Family from the Crystal Structure of PA0254 from Pseudomonas aeruginosa. *PLoS One 8*, e63161.

(13) Meganathan, R. (2001) Ubiquinone biosynthesis in microorganisms. *FEMS Microbiol. Lett. 203*, 131−139.

(14) Rangarajan, E. S., Li, Y. G., Iannuzzi, P., Tocilj, A., Hung, L. W., Matte, A., and Cygler, M. (2004) Crystal structure of a dodecameric FMN-dependent UbiX-like decarboxylase (Pad1) from Escherichia coli O157: H7. *Protein Sci. 13*, 3006−3016.

(15) Gothelf, K. V., and Jorgensen, K. A. (1998) Asymmetric 1,3-dipolar cycloaddition reactions. *Chem. Rev. 98*, 863−909.

(16) Pellissier, H. (2007) Asymmetric 1,3-dipolar cycloadditions. *Tetrahedron 63*, 3235−3285.

(17) Waugh, M. W., and Marsh, E. N. G. (2014) Solvent Isotope Effects on Alkane Formation by Cyanobacterial Aldehyde Deformylating Oxygenase and Their Mechanistic Implications. *Biochemistry 53*, 5537−5543.

(18) Pindur, U., and Schneider, H. G. (1994) Pericyclic Key Reactions in Biological Systems. *Chem. Soc. Rev. 23*, 409−415.

(19) Miyamoto, K., and Ohta, H. (1992) Purification and Properties of a Novel Arylmalonate Decarboxylase from *Alcaligenes-bronchisepticus* KU-1201. *Eur. J. Biochem. 210*, 475−481.

(20) Kurti, L., and Czako, B. (2005) *Strategic Applications of Named Reactions in Organic Synthesis*, Elsevier Academic Press.

(21) Gadda, G., and Fitzpatrick, P. F. (2013) Solvent isotope and viscosity efects on the steady state kinetics of the flavoprotein nitroalkane oxidase. *FEBS Lett. 587*, 2785−2789.

(22) Jaffe, H. H. (1953) A Reexamination of the Hammett Equation. *Chem. Rev. 53*, 191−261.

(23) Neims, A. H., Deluca, C. D., and Hellerman, L. (1966) Studies on Crystaline D-Amino Acid Oxidase. III. Substrate Specificity and sigma-pi Relationship. *Biochemistry 5*, 203−207.

(24) Yorita, K., Misaki, H., Palfey, B. A., and Massey, V. (2000) On the interpretation of quantitative structure-function activity relationship data for lactate oxidase. *Proc. Natl. Acad. Sci. U. S. A. 97*, 2480−2485.

(25) Trahanovsky, W. S., Cramer, J., and Brixius, D. W. (1974) Oxidation of Organic Compounds with Cerium(IV) 0.18. Oxidative Decarboxylation of Substittued Phenylacetic Acids. *J. Am. Chem. Soc. 96*, 1077−1081.

(26) Cleland, W. W. (1987) Secondary isotope effects on enzymatic reactions. In *Isotopes in Organic Chemistry* (Buncel, E., and Lee, C. C., Eds.) Elsevier, Amsterdam.

(27) Cleland, W. W. (2005) The use of isotope effects to determine enzyme mechanisms. *Arch. Biochem. Biophys. 433*, 2−12.

(28) Kurtz, A. K., and Fitzpatrick, P. F. (1997) pH and Secondary Kinetic Isotope Effects on the Reaction of D-Amino Acid Oxidase with Nitroalkane Anions: Evidence for Direct Attack on the Flavin by Carbanions. *J. Am. Chem. Soc. 119*, 1155−1156.

(29) Northrop, D. B. (1975) Steady-State Analysis of Kinetic Isotope Effects in Enzyme Reactions. *Biochemistry 14*, 2644−2651.

(30) Wuensch, C., Pavkov-Keller, T., Steinkellner, G., Gross, J., Fuchs, M., Hromic, A., Lyskowski, A., Fauland, K., Gruber, K., Glueck, S. M., and Faber, K. (2015) Regioselective Enzymatic beta-Carboxylation of Hydroxy-styrene Derivatives Catalyzed by Phenolic Acid Decarboxylase. *Adv. Synth. Catal. 357*, 1909−1918.

(31) Perez, P., Domingo, L. R., Aurell, M. J., and Contreras, R. (2003) Quantitative Characterization of the global electrophilicty pattern of some reagents involved in 1,3-dipolar cyclo-addition reaction. *Tetrahedron 59*, 3117−3125.

DOI: 10.1021/acs.biochem.6b00170
Biochemistry XXXX, XXX, XXX−XXX